DEVELOPMENT OF DIRECT-DETECTION DOPPLER WIND LIDAR FOR VERTICAL ATMOSPHERIC MOTION

Shoken Ishii[1,2*], Makoto Aoki[1], Kanna Tominaga[2], Tomoaki Nishizawa[3], Yoshitaka Jin[3],
Nobuo Sugimoto[3], Yasukuni Shibata[2], Atsushi Sato[4, 1], Kaori Sato[5], and Hajime Okamoto[5]

[1]National Institute of Information and Communications Technology, Koganei Tokyo 184-8795, Japan
[2]Tokyo Metropolitan University, Hino Tokyo 191-0065, Japan
[3]National Institute of Environmental Studies, Tsukuba Ibaraki 305-8506, Japan
[4]Tohoku Institute of Technology, Sendai Miyagi 982-8577, Japan
[5]Kyushu University, Kasuga Fukuoka 816-8580, Japan
**Email: sishii@nict.go.jp*

ABSTRACT

Wind is fundamental in many atmospheric phenomena. Global wind profile observation is important to improve numerical weather prediction (NWP) and various meteorological studies. Wind profile observations are measured mainly by radiosonde networks. A Doppler Wind Lidar (DWL) is a useful remote sensing technique for wind measurement. DWL would provide us with a wind profile having high vertical resolution, low bias, and good precision. The National Institute of Information and Communications Technology (NICT) studies DWL has been developing various DWL. In the paper, we report development of a 355-nm direct-detection DWL and describe recent results of a 2-µm coherent DWL at NICT.

1. INTRODUCTION

Current space-based passive observing systems for wind measurement is limited [1]. The current space-based passive observing systems have a large coverage area and high temporal and horizontal resolutions but has a low vertical resolution. The World Meteorological Organization (WMO) wants to develop space-based wind profiling systems [2]. A Doppler Wind Lidar (DWL) can provide us with a wind profile with high vertical resolution, low bias, and good precision. A space-based DWL can fill the gap for the current space-based passive observing systems. The European Space Agency (ESA) launched a first space-based DWL called 'Aeolus' for the global wind profile observation in 2018 [3]. The National Institute of Information and Communications Technology (NICT) is studying the feasibility to realize the future space-based DWL [4-6]. NICT developed a ground-based 2-µm coherent DWL for CO_2 and wind measurements [7]. We have a plan to make wind measurement around and inside clouds with 355-nm direct-detection and 2-µm coherent DWL measurements. We are developing a ground-based direct-detection DWL. In the paper, we describe development and progress of the two DWLs.

2. DEVELOPMENT of 355-NM DIRECT-DETECTION DOPPLER WIND LIDAR

2.1 355-nm direct-detection lidar system

A direct-detection DWL has the advantage that wind measurement can be made any aerosol conditions because it uses the light backscattered by molecules (Rayleigh scattering). This feature is one of the characteristics of the direct-detection DWL. NICT is developing a direct-detection DWL with a double-edge technique. Figure 1 and Table 1 show a block diagram and specifications of the direct-detection DWL. The direct-detection DWL uses a flash-lump-pumped Q-switched Nd:YAG laser (Contuinum: Surelite I), an o Schmidt-Cassegrain type (Celestron: C14), a Fabry-Perot etalon, a knife-edge right-angle prism mirror, and two photomultiplier tubes (Hamamatsu: R9880U-113), The single-frequency a flash-lump-pumped Q-switched Nd:YAG operating at a wavelength of 0.355 µm can emit an output energy of 100 mJ with a pulse width of 10 ns (FWHM) at a pulse repetition frequency of 10 Hz. The wavelength of backscattered light is Doppler-shifted from that of the incident laser light by the moving molecules and aerosols. The backscattered light is collected by a telescope and split into two paths using a wedge plate. Each split light beam passes through a Fabry-Perot étalon (which functions as an edge filter) and is focused on each detector. The number of photons, $N_{i=1,2}$ detected at each detector for a line-of-sight (LOS) wind speed of v_{LOS} (m/s) is given as Eq. (1),

$$N_{s,i}(v_{LOS}) = T_{BS}\cdot\frac{E_T\cdot Freq\cdot\Delta t}{h\nu_L}\cdot A_T\cdot T_O\cdot O_A(r)\cdot Q_e\cdot\frac{\Delta r}{r^2}\cdot {T_A}^2 \times\left[\beta_M(r)\cdot\int_{-\infty}^{\infty}T_{F,\,i}(\nu)\cdot\{G_L*G_M(\nu,\Delta\nu)\}d\nu+\beta_A(r)\cdot\int_{-\infty}^{\infty}T_{F,\,i}(\nu)\cdot\{G_L*L_A(\nu,\Delta\nu)\}d\nu\right], \quad (1)$$

where T_{BS} is the beam-splitter transmittance, E_T is the transmitted laser energy, Freq is a pulse repetition frequency, Δt is integration time, ν_L is the laser frequency, A_T is the telescope area, T_o is optical efficiency of the system without etalon transmission, $O_A(r)$ is an overlap function, Q_e is quantum efficiency of the detector, Δr is range bin length, r is a distance to the target atmosphere, T_A is atmospheric transmission, $T_{F,i=1,2}(\nu)$ is transmission at a frequency of ν for an edge filter centered at ν_L, β_m and β_a are the molecule and aerosol backscattering coefficients, G_L and G_m are Gaussian line-broadening functions for the laser-line spectrum and the Rayleigh-Brillouin spectrum, L_a is a Lorentzian function for the aerosol-line spectrum, Δν is the Doppler-shifted frequency, the asterisk denotes a convolution operation, 'h' is Planck's constant, and 'c' is the light speed.

Since the photon noise is the dominant noise source, we assume that the standard deviation of N_i is given by a Poisson distribution. SNR_i is given as Eq. (2),

$$SNR_i = \sqrt{Freq\cdot\Delta t}\cdot\frac{N_i/Freq\cdot\Delta t}{\sqrt{N_i/Freq\cdot\Delta t+N_{DC}+N_{BG}}}, \quad (2)$$

where N_{DC} and N_{BG} are the dark current noise of the detector and the background noise. The location of the *i*th edge filter is determined by the following condition described by Flesia and Korb [8]. the LOS wind speed error σ_{LOS} is given by

$$\sigma_{LOS} = \frac{c}{\frac{2}{v}\cdot\left(\frac{1}{N_1(0)}\frac{d}{dv}N_{s,M,1}(0)+\frac{-1}{N_2(0)}\frac{d}{dv}N_{s,M,2}(0)\right)}\cdot\sqrt{\frac{1}{SNR_1^2}+\frac{1}{SNR_2^2}}. \quad (3)$$

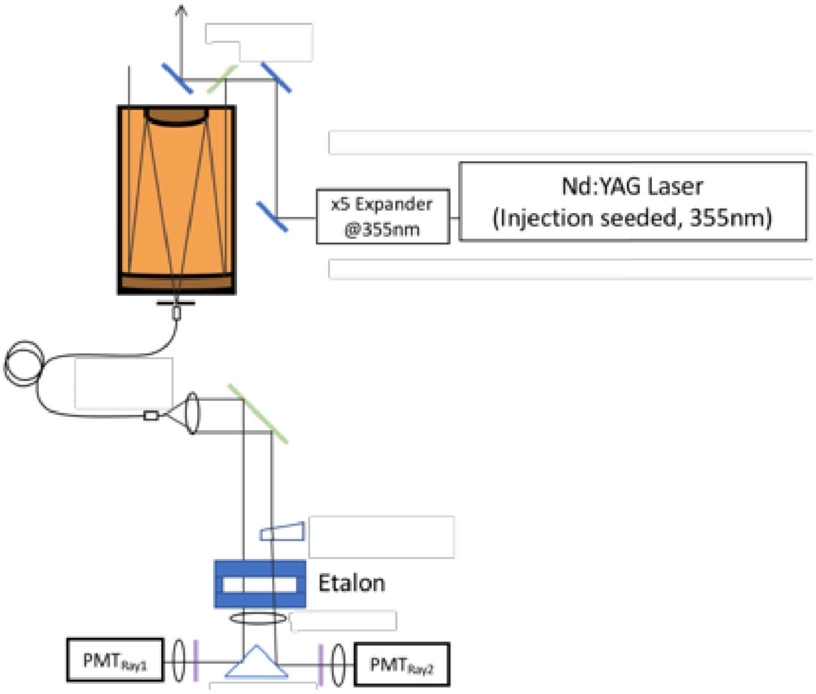

Figure 1. Block diagram of 355-nm direct-detection Doppler wind lidar.

Table 1. Specifications of 355-nm direct-detection Doppler wind lidar.

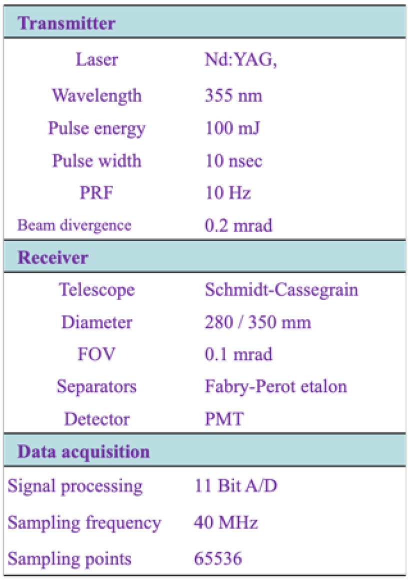

Transmitter	
Laser	Nd:YAG,
Wavelength	355 nm
Pulse energy	100 mJ
Pulse width	10 nsec
PRF	10 Hz
Beam divergence	0.2 mrad
Receiver	
Telescope	Schmidt-Cassegrain
Diameter	280 / 350 mm
FOV	0.1 mrad
Separators	Fabry-Perot etalon
Detector	PMT
Data acquisition	
Signal processing	11 Bit A/D
Sampling frequency	40 MHz
Sampling points	65536

2.2 Wind Measurement performance of 355nm direct-detection DWL

Figure 2 shows the profile of the LOS wind error calculated from Eqs (1) through (3) for a LOS wind speed of 1 m/s for the various accumulation laser pulse: 100, 600, 3000, and 6000. The figure shows that altitudes for the LOS wind speed errors of 0.5 m/s for the four accumulation laser pulses are 2, 5, 10, and 15 km. Our coherent lidar developed for and wind measurements can make vertical wind speed measurement at altitudes up to about 10 km for the accumulation laser pulse of 30 corresponding to 1 sec, where depends on the load of aerosol or clouds. When SNR is high, the 2-µm coherent lidar can make wind measurement with random error of 0.12 m/sec and vert low bias of <0.1 m/sec under the real atmospheric conditions [9]. The appropriate accumulation laser pulses for the dual DWL measurements are 100 and 600 shots.

3. VERTICAL WIND MEASUREMENT PERFORMANCE OF 2-µM COHERENT DOPPLER WIND LIDAR

A ground-based 2-µm coherent DWL was developed at NICT in 2013. The block diagram specifications of the ground-based coherent DWL are shown in Figure 3 and Table 2, respectively. The ground-based DWL uses a conductively-cooled laser-diode-pumped Q-switched Tm,Ho:YLF laser, an off-axis telescope, two heterodyne detectors, and signal processing devices. The single-frequency Q-switched Tm,Ho:YLF laser an emit an output energy of 90 mJ with a pulse width of 150 ns (FWHM) at a pulse repetition frequency of 40 Hz. The bias and error in the LOS wind speed measurement were also investigated by returns backscattered from a building (hard target) located at about 25 km. The ground-based coherent DWL can make the LOS wind speed with a low bias of <0.0 m/sec and random error of about 0.1 m/sec estimated from 10-shot averaged zero LOS wind speeds. Figure 4 shows the vertical wind speed measurements of atmosphere, aerosols and clouds by the ground-based coherent DWL at NICT headquarters on 27 March 2018. The ground-based coherent DWL detected details of thermal convections near in the atmospheric boundary layer.

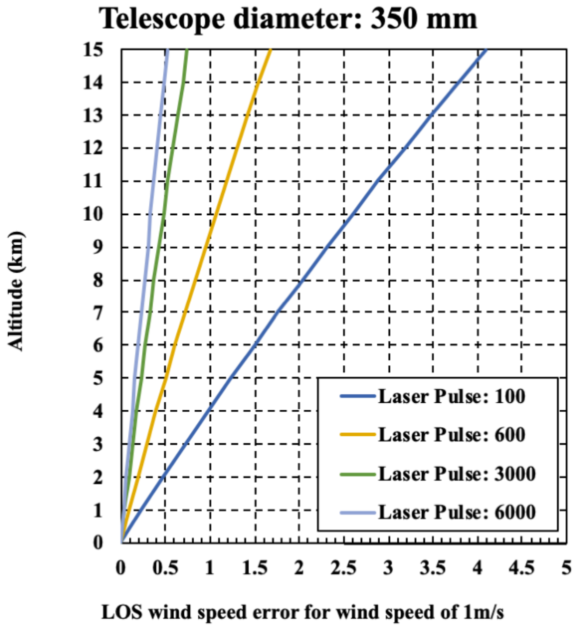

Figure 2. Profiles of the LOS wind speed error for various accumulation laser pulse:100, 600, 3000, and 6000.

4. SUMMARY

A DWL is a useful remote sensing technique for wind measurement. DWL would provide us with a wind profile with high vertical resolution, low bias, and good precision. We have plan to make vertical wind measurement around and in side clouds with

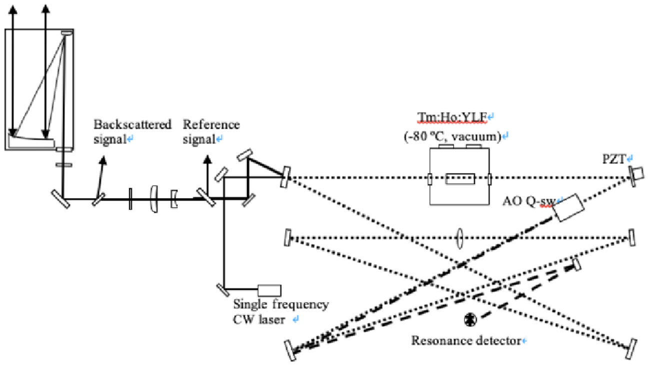

Figure 3. Block diagrams of 2-μm coherent Doppler wind lidar.

Table 2. Specifications of 2-μm coherent Doppler wind lidar.

Transmitter	
Laser	Tm,Ho:YLF
Wavelength	2051.002–2051.058 nm (On) 2051.250 nm (Off)
Pulse energy	50–80 mJ/pulse (Target)
Pulse width	150 ns (FWHM)
Pulse repetition	> 30 Hz
Polarization	Circular
Receiver	
Telescope type	Mersenne off-axis
Diameter	10 cm
Magnification	10 x
Detector	InGaAs-PIN photodiode
DET$_1$	Balanced InGaAs-PIN photodiode
Resolution	14-bit A/D conversion
Sampling frequency	400 MHz

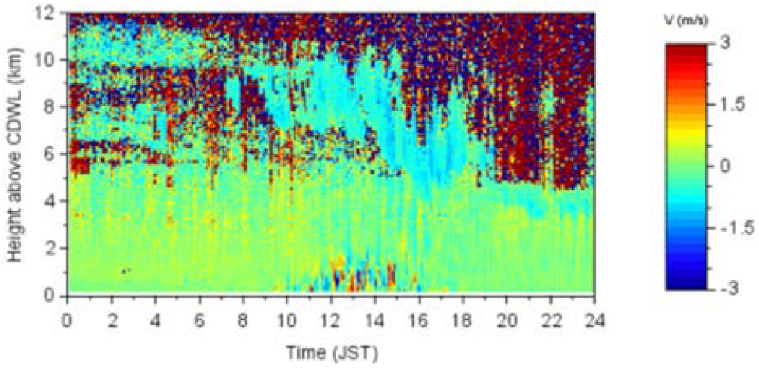

Figure 4. Temporal variation of vertical wind speed and SNR observed by 2-μm coherent DWL on 27 Mach, 2018.

direct-detection and coherent DWL wind measurements. NICT is a developing a direct-detection DWL with the double-edge technique. Our result shows that the appropriate accumulation laser pulses of 100 and 600 shots is appropriate for the direct-detection DWL wind measurement. The 2-μm coherent DWL can describe temporal variation of atmosphere. The combination of direct-detection and coherent DWL wind measurement would be useful for investigating details of various motions in the atmosphere. The dual DWL wind measurements with a cloud radar measurement. would be suitable to evaluate and characterize vertical wind motion around and inside clouds.

ACKNOWLEDGEMENTS

This research is supported by JSPS KAKENHI under Grant Numbers JP17H06139. A part of this research was supported by the Collaborated Research Program of Research Institute for Applied Mechanics, Kyushu University.

REFERENCES

[1] W. E. Baker et al. Bull. Am. Meteorol. Soc., 95, 543-564 (2014).
[2] WMO. WMO Tech. Rep. 2012-1, 6 (2012).
[3] ESA. SP-1233(4), (1999).
[4] S. Ishii et al. J. Meteorol. Soc. Jpn.95, 301-317 (2017).
[5] P. Baron et al. J. Meteorol. Soc. Jpn 95, 319-342 (2017).
[6] K. Okamoto et al. J. Meteorol. Soc. Jpn. 96, 179-199 (2018).
[7] S. Ishii et al. Appl. Opt., 49, 1809-1817 (2010).
[8] Flesia and Korb, Appl. Opt. **38**, 432-440 (1999).
[9] Iwai et al. J. Atmos. Ocean. Technol., 30(3), 429-449 (2013).